Substituted Polyfluorene-Based Hole Transport Layer with Tunable Solubility

Craciun, N. I.; Wildeman, J.; Blom, P. W. M.

Published in:
Journal of Physical Chemistry C

DOI:
10.1021/jp101079y

Publication date:
2010

Substituted Polyfluorene-Based Hole Transport Layer with Tunable Solubility

N. I. Craciun,[†] J. Wildeman,[†] and P. W. M. Blom*[,†,‡]

Molecular Electronics, Zernike Institute for Advanced Materials, University of Groningen, Nijenborgh 4, 9747 AG Groningen, The Netherlands, and TNO/Holst Centre, High Tech Campus 31, 5605 KN Eindhoven, The Netherlands

Received: February 4, 2010; Revised Manuscript Received: May 4, 2010

We report on the synthesis and electrical characterization of polyfluorene−triarylamine-based hole transport layers (HTLs). The solubility of the HTL can be tuned by adjustment of the chemical structure without loss of the charge transport properties. Double-layer polymer light-emitting diodes are constructed with an HTL that is not soluble in toluene at room temperature, combined with a poly(*p*-phenylene vinylene) (PPV)-derivative-based light-emitting layer. The addition of the HTL enhances the efficiency of the PLED with 10% at higher voltages.

1. Introduction

Organic light-emitting diodes (OLEDs) are considered to be promising candidates for applications, ranging from lighting to full-color emissive displays. Basically, an organic LED consists of a thin organic electroluminescent layer sandwiched between two electrodes. Organic LEDs are typically made from either small molecules[1] or from conjugated polymers.[2] Small-molecule-based devices are deposited with vacuum techniques, whereas soluble conjugated polymers are processed from solution. An advantage of evaporated small-molecule-based devices is that the active part consists of various layers with different functions, leading to highly efficient devices.[3] These layers are chosen to have properties such as hole and electron transport, hole or electron blockage and high emission. Wet-processing techniques are more suited than vacuum deposition in terms of roll-to-roll processing of organic electroluminescent materials onto flexible plastic substrates. The active part of present state-of-the-art polymeric light-emitting diodes (PLEDs) consists of only a single layer. In such a device, holes are injected from the anode and electrons from the cathode into the polymer layer. The use of only a single electro-optic layer has a large fundamental disadvantage: because of the reduced electron transport in conjugated polymers, most of the light in a PLED is generated close to the metallic cathode. This metallic cathode acts as a quenching site for the generated excitons, thereby strongly reducing the efficiency of the PLEDs. These fundamental limitations can be circumvented by using devices consisting of a number of active layers. In such a heterojuction device, electrons and holes cannot leave the device without recombining, as has been demonstrated for OLEDs based on evaporated small molecules with a nearly 100% internal quantum efficiency.[4] A major problem for polymer-based multilayer devices is the solubility of the materials used; a multilayer can not be fabricated when a spin-casted layer dissolves in the solvent of the subsequent layer.

In recent years, a number of approaches have been developed to realize solution processed multilayer PLEDs. A first approach efficient double layer has been realized using a precursor poly(phenylene vinylene) (PPV) as a hole transport layer (HTL).[5] In one approach, orthogonal solvents are used for the construction of organic multilayers: by subsequently depositing materials that can be dissolved in polar and nonpolar solvents, a three-layer polymer LED was fabricated.[6] The success of the approach of using orthogonal solvents depends on the ability to reproducibly synthesize materials with the required solubility and to maintain good optical and electrical properties. An alternative approach is the use of cross-linkable materials in layers of the organic LED to be able to prevent redissolving during deposition of subsequent layers.[7−9] Cross-linking is induced by ultraviolet (UV) exposure, comparable to standard photoresist. To enable cross-linking, it is necessary to have monomers/prepolymers with reactive groups. These groups, however, can have a negative effect on the charge transport and luminescence properties. For cross-linking, the challenge is to achieve long lifetime of the devices because excess material from the cross-linking process may remain in the device. Another technique for obtaining multilayer structures is to use a liquid buffer layer during processing, as reported for a polymer-based multilayer OLED.[10] The buffer layer of (1,2-propylene glycol), which does not dissolve in the solvents of the polymers, is deposited on top of the first polymer layer. The second polymer layer then initially floats on the buffer layer until the buffer layer evaporates, during either the deposition process or a baking step. A challenge here is that some (1,2-propylene glycol) may remain in the device structure and degrade performance. As a final approach, the use of poly(2,7-(9,9-di-*n*-octylfluorene)-*alt*-(1,4-phenylene-((4-*s*-butylphenyl)imino)-1,4-phenylene)) (TFB) as an interlayer between poly(3,4-ethylenedioxythiophene) (PEDOT) and the light-emitting layer is reported. The TFB layer is hard baked at temperatures in the range of 180 °C before the second polymer layer is deposited from an organic solvent.[11] It has been observed that for a TFB layer that was originally 70 nm thick, only 8−10 nm has been lost after it has been in contact with the second solvent-based layer.[12]

Another approach is to tune the solubility by chemical modification;[13] copolymers with selective solubility can be achieved without the loss of the enhanced charge transport properties. It was shown that by shortening the (2′-ethylhexyloxy) side chains, from poly[2,5-bis(2′ethylhexyloxy)-1,4-phenylenevinylene] (BEH-PPV), to butoxy side chains, the polymer

* Corresponding author.
[†] University of Groningen.
[‡] TNO/Holst Centre.

10.1021/jp101079y
Published on Web 05/21/2010

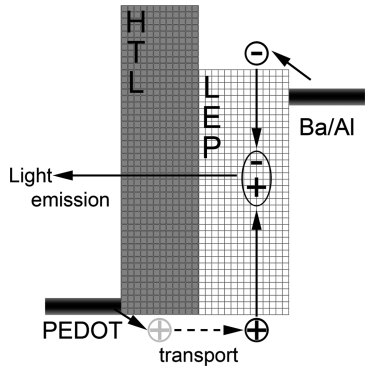

Figure 1. Schematic representation of a double-layer PLED with a hole transport layer (HTL) that blocks electrons and a light-emitting polymer (LEP). The double-layer PLED is sandwiched between an Ohmic PEDOT/PSS contact and a Ba/Al cathode.

poly[2,5-bis(butoxy)-1,4-phenylenevinylene] (BB-PPV) was obtained, which is only soluble in chloroform in very low concentrations. Consequently, by tuning the ratio of the BEH and BB monomers, we could adjust the solubility over the whole spectrum of solvents, thereby preserving the enhanced charge transport properties. For example, an HTL of a BEH-BB-PPV copolymer in 1:3 ratio was only soluble in chloroform, making it compatible with a large number of light-emitting polymers (LEPs). However, a disadvantage of these PPV-based double-layer PLEDs is that the HOMO and LUMO levels of the HTL and LEP align, such that the electrons are not blocked at the interface. In an improved double-layer device, the HTL should have a larger band gap than the LEP. At the same time, the HOMO levels of these two polymers have to align to inject holes from the HTL into the LEP efficiently, as schematically shown in Figure 1. Furthermore, the chemical structure of the HTL has to be designed in such a way that when the LEP layer is spin-coated on top, it will not be dissolved (Figure 1).

In this article, we report the development of wide band gap poly(9,9-dioctylfluorene (PFO)−triarylamine-based HTLs with a tunable solubility. The solubility can be adjusted by modification of the chemical structure, which enables the construction of a heterojunction with electron blocking functionality.

2. Experimental Section

Synthesis of Poly(9,9-dioctyl-9*H*-fluorene-2,7-diyl)-*co*-(*N*4,*N*4′-bis(*p*-phenylene)-*N*4,*N*4′-bis(4-(2-ethylhexyloxy)phenyl)biphenyl-4,4′-diamine) (PFO-BEHTPD). Under a nitrogen atmosphere, 216 mg (0.34 mmol) of 2,2′-(9,9-dioctyl-9*H*-fluorene-2,7-diyl)bis(4,4,5,5-tetramethyl-1,3,2-dioxaborolane) (Figure 2a), 307 mg (0.34 mmol) of *N*,*N*-di(4-ethylhexylphenyl)-*N*,*N*-bis(4-bromophenyl)-[1,1′-biphenyl]-4,4′-diamine (Figure 2b), 8 mg (0.007 mmol) of tetrakis(triphenylphoshine)palladium (0), toluene (10 mL), KOH solution (4 mL, 20%), and 13.5 mg of TBABr (ca. 0.04 mmol) were placed in a round-bottomed flask and stirred vigorously at refluxed temp for 4 h. The reaction mixture was precipitated in 40 mL of methanol and stirred for 0.5 h. The solid green-yellow material was washed with methanol and acetone and isolated on a Buchner filter. The polymer was dried in air. The yield was 350 mg, 93%. We further purified the polymer by dissolving it in 4 mL of toluene, and it was precipitated in acetone (50 mL), affording 335 mg of pure PFO-BEHTPD (Figure 2c).

Synthesis of Poly(9,9-dioctyl-9*H*-fluorene-2,7-diyl)-*co*-(*N*4,*N*4′-bis(*p*-phenylene)-*N*4,*N*4′-diphenylbiphenyl-4,4′-diamine) (PFO-TPD). Under a nitrogen atmosphere, 321.3 mg (0.5 mmol) of 2,2′-(9,9-dioctyl-9*H*-fluorene-2,7-diyl)bis(4,4,5,5-tetramethyl-1,3,2-dioxaborolane) (Figure 3a), 323.2 mg (0.5 mmol) of *N*,*N*-diphenyl-*N*,*N*-bis(4-bromophenyl)-[1,1′-biphenyl]-4,4′-diamine (Figure 3b), 9 mg (0.008 mmol) of tetrakis(triphenylphoshine)palladium (0), toluene (10 mL), KOH solution (5 mL, 20%), and 17 mg of TBABr (ca. 0.05 mmol) were placed in a round-bottomed flask and stirred vigorously at refluxed temp for 4 h. (After 1 h, a lump of sticky material was already observed.) The reaction mixture was diluted with ca. 30−40 mL chloroform (gel-like material), precipitated in 400 mL of methanol, and stirred for 0.5 h. The formed precipitate was washed with methanol and isolated on a Buchner filter. The polymer was dried, affording 418 mg, 95% of crude polymer (Figure 3c). The crude polymer was redissolved in hot dichlorobenzene (40 mL) and reprecipitated from acetone. The refined polymer was isolated on a filter and dried in vacuum at room temperature. The yield was 780 mg, 90%. The molecular weight of 20.000 g/mol was determined with NMR.

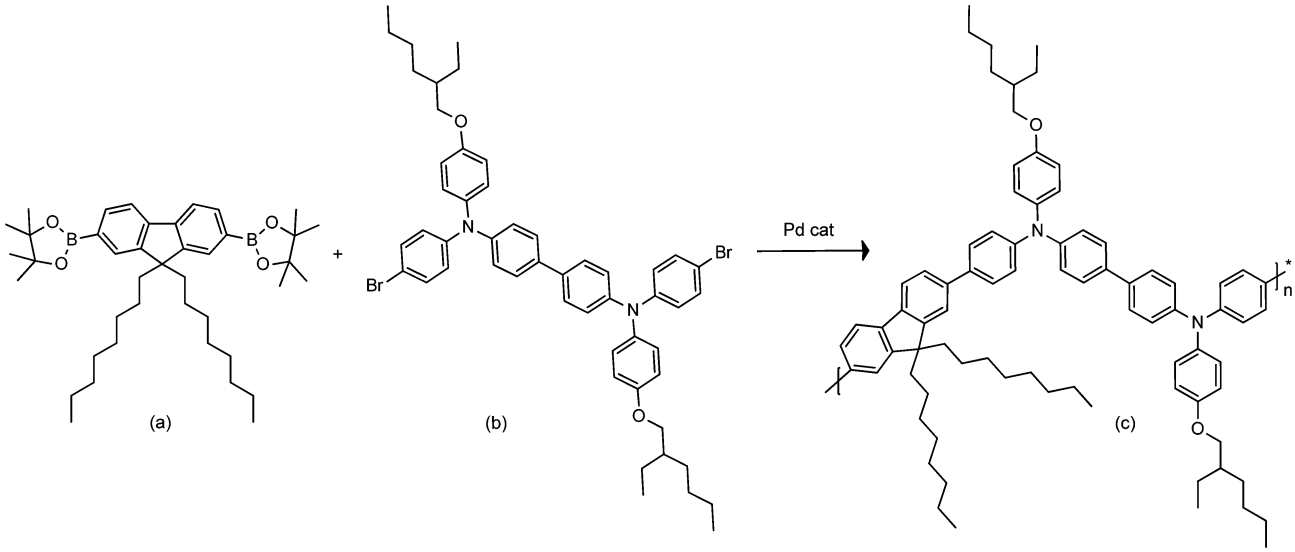

Figure 2. Synthesis of PFO-BEHTPD (c). (a) 2,2′-(9,9-Dioctyl-9*H*-fluorene-2,7-diyl)bis(4,4,5,5-tetramethyl-1,3,2-dioxaborolane). (b) *N*,*N*-di(4-Ethylhexylphenyl)-*N*,*N*-bis(4-bromophenyl)-[1,1′-biphenyl]-4,4′-diamine.

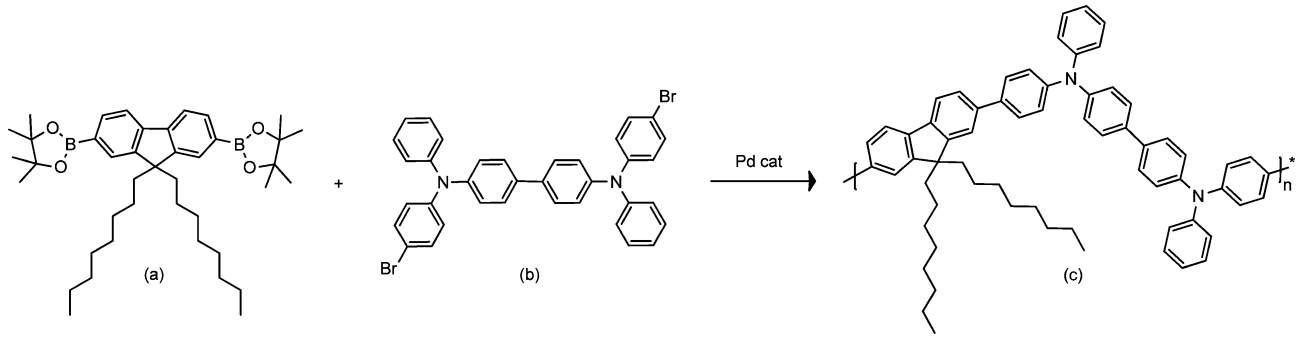

Figure 3. Synthesis of PFO-TPD (c). (a) 2,2′-(9,9-Dioctyl-9*H*-fluorene-2,7-diyl)bis(4,4,5,5-tetramethyl-1,3,2-dioxaborolane). (b) *N*,*N*-Diphenyl-*N*,*N*-bis(4-bromophenyl)-[1,1′-biphenyl]-4,4′-diamine.

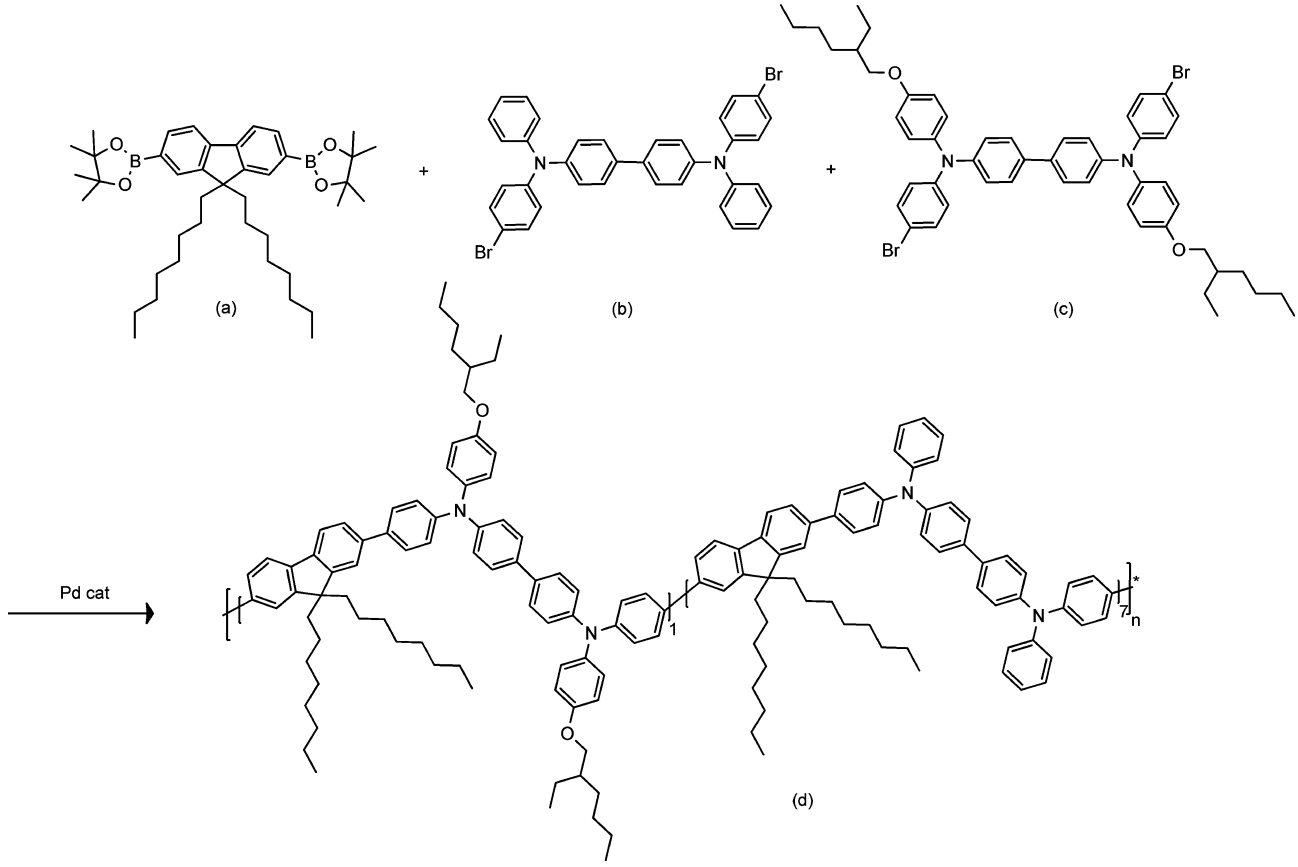

Figure 4. Synthesis of [PFO-BEHTPD]$_1$[PFO-TPD]$_7$ (d). (a) 2,2′-(9,9-Dioctyl-9*H*-fluorene-2,7-diyl)bis(4,4,5,5-tetramethyl-1,3,2-dioxaborolane). (b) *N*,*N*-Diphenyl-*N*,*N*-bis(4-bromophenyl)-[1,1′-biphenyl]-4,4′-diamine. (c) *N*,*N*-di(4-Ethylhexyloxyphenyl)-*N*,*N*-bis(4-bromophenyl)-[1,1′-biphenyl]-4,4′-diamine.

Synthesis of Poly[(9,9-dioctyl-9*H*-fluorene-2,7-diyl)-*co*-(*N*4,*N*4′-bis(*p*-phenylene)-*N*4,*N*4′-bis(4-(2-ethylhexyloxy)phenyl)biphenyl-4,4′-diamine)]$_1$ *ran*-[(9,9-Dioctyl-9*H*-fluorene-2,7-diyl)-*co*-(*N*4,*N*4′-bis(*p*-phenylene)-*N*4,*N*4′-diphenylbiphenyl-4,4′-diamine)]$_7$ [PFO-BEHTPD]$_1$[PFO-TPD]$_7$. Under a nitrogen atmosphere, 282 mg (0.44 mmol) of 2,2′-(9,9-dioctyl-9*H*-fluorene-2,7-diyl)bis(4,4,5,5-tetramethyl-1,3,2-dioxaborolane) (Figure 4a), 248,5 mg (0.385 mmol) of *N*,*N*-diphenyl-*N*,*N*-bis(4-bromophenyl)-[1,1′-biphenyl]-4,4′-diamine (Figure 4b), 45.5 mg (0.055 mmol) of *N*,*N*-di(4-ethylhexyloxyphenyl)-*N*,*N*-bis(4-bromophenyl)-[1,1′-biphenyl]-4,4′-diamine (Figure 4c), 10 mg (0.009 mmol) of tetrakis(triphenylphoshine)palladium (0), toluene (12 mL), KOH solution (5 mL, 20%), and 16 mg of TBABr (ca. 0.05 mmol) were placed in a round-bottomed flask and stirred vigorously at refluxed temp for 3 h. We worked up the reaction mixture by precipitating it in 40 mL of methanol, and it was stirred for 0.5 h. The solid material was washed with methanol and acetone and isolated on a Buchner filter. The polymer was dried in air. The yield was 385 mg, 90%. We further purified the polymer by dissolving it in 15 mL of hot toluene and precipitated it in acetone (75 mL), affording 345 mg of pure random copolymer (Figure 4d).

Device Fabrication. To characterize the hole transport, we fabricated hole-only diodes from both PFO-BEHTPD and [PFO-BEHTPD]$_1$[PFO-TPD]$_7$. These hole-only diodes are prepared as follows: on top of a glass substrate, a transparent electrode, indium−tin oxide (ITO), has been patterned to form the hole injecting electrode. Subsequently, an anode of the hole-conducting polymer, poly(3,4-ethylenedioxythiophene)/poly-(styrenesulfonate) (PEDOT/PSS), is spin coated. Then, on top of the PEDOT/PSS, PFO-BEHTPD or [PFO-BEHTPD]$_1$[PFO-TPD]$_7$ films have been spin coated from hot toluene (70 °C) solutions. The devices were finished by thermal evaporation of 100 nm of gold (Au) through a shadow mask. Au has a high

work function that does not inject electrons into the polymer. The hole-only diodes have been measured under a controlled N_2 atmosphere. The electrical measurements have been performed using a Keithley 2400 SourceMeter. It should be mentioned that [PFO-BEHTPD]$_1$[PFO-TPD]$_7$ is soluble only in hot toluene, and it becomes insoluble in toluene at room temperature. For the double-layer PLEDs, MEH-PPV was spin coated on top of the PFO-based HTL as the light-emitting layer from toluene at room temperature.

3. Results and Discussion

For a basic compound for the wide band gap HTL, we started with the blue-emitting PFO, which has a band gap of 3.2 eV.[14] However, because of its deep HOMO level of 5.8 eV, it is very difficult to inject holes in PFO efficiently.[15] To lift the HOMO level, PFO has been functionalized with triarylamine-based units. These dioctylfluorene−triarylamine conjugated copolymers combine the excellent hole transport properties of the triarylamines with the processability of conjugated polymers.[14] Furthermore, because of the decrease in the ionization potential, typically from 5.8 eV for PFO to ∼5.0 eV for the copolymers, the hole injection from standard anodes as PEDOT/PSS is very efficient.[15] In this study, we combined the 2,2′-(9,9-dioctyl-9*H*-fluorene-2,7-diyl)bis(4,4,5,5-tetramethyl-1,3,2-dioxaborolane) monomer (Figure 2a) with *N*,*N*-di(4-ethylhexylphenyl)-*N*,*N*-bis(4-bromophenyl)-[1,1′-biphenyl]-4,4′-diamine (Figure 2b), resulting in poly(9,9-dioctyl-9*H*-fluorene-2,7-diyl)-*co*-(N4,N4′-bis(*p*-phenylene)-*N*4,*N*4′-bis(4-(2-ethylhexyloxy)phenyl)biphenyl-4,4′-diamine) (PFO-BEHTPD) (Figure 2c). As a next step, the solubility of the PFO-BEHTPD, which is soluble in a large amount of solvents, has to be tuned to make it suited as an HTL in a solution-processed PLED. For this purpose, the 2,2′-(9,9-dioctyl-9*H*-fluorene-2,7-diyl)bis(4,4,5,5-tetramethyl-1,3,2-dioxaborolane) (Figure 3a) was combined with *N*,*N*-diphenyl-*N*,*N*-bis(4-bromophenyl)-[1,1′-biphenyl]-4,4′-diamine (Figure 3b), leading to poly(9,9-dioctyl-9*H*-fluorene-2,7-diyl)-*co*-(*N*4,*N*4′-bis(*p*-phenylene)-*N*4,*N*4′-diphenylbiphenyl-4,4′-diamine) (PFO-TPD) (Figure 3c), which is an insoluble polymer because of the absence of side groups on the phenyl units. A tunable solubility can be achieved by copolymerization of these two polymers, resulting in the random copolymer poly[(9,9-dioctyl-9*H*-fluorene-2,7-diyl)-*co*-(*N*4,*N*4′-bis(*p*-phenylene)-*N*4,*N*4′-bis(4-(2-ethylhexyloxy)phenyl)biphenyl-4,4′-diamine)]$_x$ *ran*-[(9,9-dioctyl-9*H*-fluorene-2,7-diyl)-*co*-(*N*4,*N*4′-bis(*p*-phenylene)-*N*4,*N*4′-diphenylbiphenyl-4,4′-diamine)]$_y$ ([PFO-BEHTPD]$_x$[PFO-TPD]$_y$) (Figure 4d). For a ratio of 1:7, ([PFO-BEHTPD]$_x$[PFO-TPD]$_y$) becomes insoluble in toluene at room temperature, but it is still soluble when the solution is heated at temperatures >70 °C.

As a next step, we characterized the hole transport properties of the dioctylfluorene−triarylamine copolymers. Hole-only diodes were fabricated from PFO-BEHTPD and [PFO-BEHTPD]$_1$[PFO-TPD]$_7$ using patterned indium−tin oxide (ITO) on top of a glass substrate, followed by spin coating of a hole-injection layer of (PEDOT/PSS). Then, PFO-BEHTPD or [PFO-BEHTPD]$_1$[PFO-TPD]$_7$ films were spin coated from a hot toluene (70 °C) solution. The devices were finished by thermal evaporation of 100 nm of gold (Au) through a shadow mask. The hole-only diodes have been measured under controlled N_2 atmosphere using a Keithley 2400 SourceMeter. First, the hole mobility of the well-soluble PFO-BEHTPD is investigated. From previous studies on derivatives of poly(*p*-phenylene vinylene) (PPV), it has been demonstrated that the hole transport is space-charge limited (SCLC) with a hole mobility, μ_h, of 5×10^{-11} m^2/V s at low voltages at room temperature.[16] The enhancement of the SCL current at higher voltages was initially attributed to the electric field dependence of the mobility, originating from the lowering of the hopping barriers in the direction of the applied electric field. Recently, the dependence of the hole mobility on the charge carrier density in PPV derivatives has also been investigated by a combined study on field-effect transistors and polymeric diodes.[17] It was demonstrated that the hole mobility is constant for charge carrier densities $<10^{22}$ m^{-3} and increases with a power law for densities $>10^{22}$ m^{-3}. These experiments revealed that for a complete description of the charge transport in conjugated polymers, the effects of both carrier density and electric field on the mobility have to be taken into account.[18] Furthermore, it has recently been demonstrated that the mobility obtained from SCL polymeric diodes is enhanced by diffusion of charge carriers from an Ohmic contact into the device.[19] In Figure 2, the experimental $J-V$ measurements for the PFO-BEHTPD hole-only diodes with a thickness of 300 nm are shown (symbols). The applied voltage is corrected for the built-in voltage, V_{bi}. The solid lines represent the calculated $J-V$ characteristics using a device model taking drift, diffusion, and the density-dependent mobility into account.[20] At room temperature, from the analysis of the $J-V$ characteristics, we find a hole mobility at low electric fields of $1.2 \times 10^{-10}$$m^2$/(V s), which is two times higher as compared with the mobilities reported for PPV. The temperature dependence of the measured low-field mobility $\mu_h(E = 0,T)$ of PFO-BEHTPD is shown in the inset of Figure 5; it follows an Arrhenius-like temperature dependence $\mu_h(E = 0,T) = \mu_0 \exp(-\Delta/kT)$, with an activation energy of 0.44 eV. The mobility μ_0 extrapolated to $T \rightarrow \infty$ amounts to $\mu_0 = 30 \pm 10$ cm^2/(V s). As a result, the transport in PFO-BEHTPD also follows the universal behavior between activation energy and mobility, as recently reported for a whole range of conjugated polymers.[21]

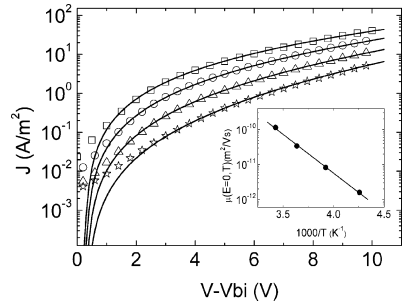

Figure 5. Temperature-dependent $J-V$ characteristics of a PFO-BEHTPD hole-only diode (symbols) with polymer thicknesses $L = 300$ nm. The solid lines represent the calculations from a drift−diffusion transport model that takes into account the presence of holes at zero bias due to diffusion from the Ohmic contact, combined with a density dependent hole mobility. The inset shows the zero-field mobility as a function of temperature.

Subsequently, the hole mobility of [PFO-BEHTPD]$_1$[PFO-TPD]$_7$ is investigated. An important question is whether the modification of the solubility is of influence on the charge transport properties. In Figure 6, the experimental $J-V$ measurements for the [PFO-BEHTPD]$_1$[PFO-TPD]$_7$ hole-only diodes with a thickness of 420 nm are shown (symbols). From the analysis of the $J-V$ characteristics, a zero-field hole mobility of $1.0 \times 10^{-10}$$m^2$/(V s) has been found, which is very close to the mobility of PFO-BEHTPD. This shows that the mobility of the polymer does not change by the copolymerization with the insoluble PFO-TPD. Furthermore, we verified that the temperature dependence of the mobility was also identical. To make a double-layer device, an LEP has to be spin-coated on top of

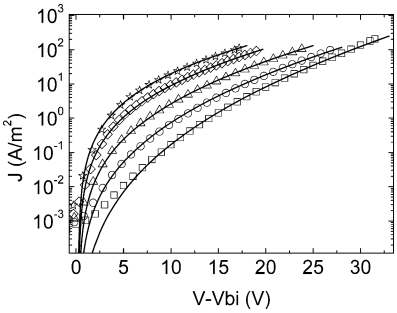

Figure 6. Temperature-dependent $J-V$ characteristics of [PFO-BEHTPD]$_1$[PFO-TPD]$_7$-based hole-only diodes (symbols) with a polymer thickness of $L = 420$ nm. The solid lines represent the calculations from the drift−diffusion model.

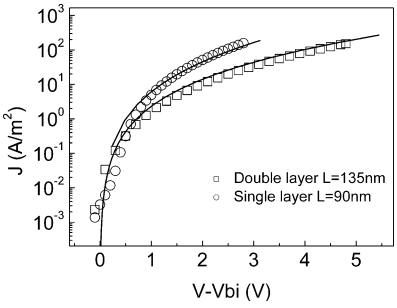

Figure 7. $J-V$ characteristics of a single-layer MEH-PPV and double-layer [PFO-BEHTPD]$_1$[PFO-TPD]$_7$/MEH-PPV hole-only diodes (symbols) at room temperature. The solid lines are the model calculations from a drift-diffusion model.

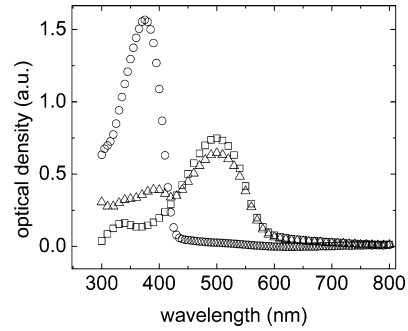

Figure 8. Optical density over wavelength for MEH-PPV (□), [PFO-BEHTPD]$_1$[PFO-TPD]$_7$ (○), and the double-layer (△).

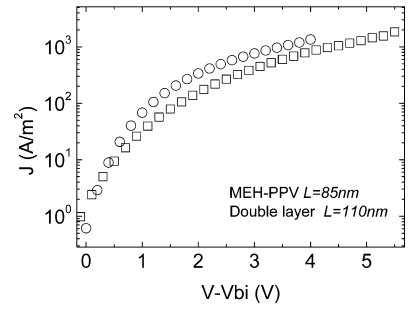

Figure 9. $J-V$ characteristics of a standard PEDOT−PSS/MEH-PPV/Ba/Al PLED (○) together with a PEDOT−PSS/[PFO-BEHTPD]$_1$[PFO-TPD]$_7$/MEH-PPV/Ba/Al (□) double-layer PLED at room temperature. The thickness of the [PFO-BEHTPD]$_1$[PFO-TPD]$_7$ layer amounts to 30 nm, and the thickness of the MEH-PPV layer is 85 nm in both devices.

the [PFO-BEHTPD]$_1$[PFO-TPD]$_7$ HTL at room temperature. We choose as a light-emitting polymer-methoxy, 5-(2′ ethylhexyloxy)-*p*-phenylene vinylene) (MEH-PPV) because it is a well characterized polymer of which the charge transport properties are well known.[19] Furthermore, with an average HOMO level of 5.1 eV and a LUMO level of 2.7 eV,[22] MEH-PPV is a suitable candidate for the second polymer layer because it is expected that holes can be easily injected from the [PFO-BEHTPD]$_1$[PFO-TPD]$_7$ into the MEH-PPV because there is no energy offset between the HOMO levels. The MEH-PPV was dissolved in toluene and spin coated at room temperature. As a reference, in Figure 7, the $J-V$ characteristics of a hole-only device consisting of a single layer MEH-PPV of 90 nm at room temperature are shown, together with the double-layer [PFO-BEHTPD]$_1$[PFO-TPD]$_7$/MEH-PPV. The thickness of the polymer layers in the double layer are 50 nm for [PFO-BEHTPD]$_1$[PFO-TPD]$_7$ and 85 nm for MEH-PPV, as obtained from thickness measurements using a DEKTAK profilometer. The MEH-PPV in both single- and double-layer devices is spin coated from the same solution so that a direct comparison between the devices can be made. From the modeling of the single layer MEH-PPV device, we obtained a zero-field room temperature of 3.0×10^{-11} m^2/(V s). With the mobility of MEH-PPV and [PFO-BEHTPD]$_1$[PFO-TPD]$_7$ now known, we can predict the $J-V$ characteristics of the double-layer device. The predicted $J-V$ characteristic is in very good agreement with the experimental data, as shown in Figure 7. This demonstrates that the thickness of the [PFO-BEHTPD]$_1$[PFO-TPD]$_7$ is not affected by spin coating the MEH-PPV on top.

Finally, a PEDOT/[PFO-BEHTPD]$_1$[PFO-TPD]$_7$/MEH-PPV/Ba/Al double-layer PLED was fabricated. The thickness of the polymer layers are 30 nm for the [PFO-BEHTPD]$_1$[PFO-TPD]$_7$ and 85 nm for the MEH-PPV. We applied only a thin [PFO-BEHTPD]$_1$[PFO-TPD]$_7$ HTL to limit the voltage drop across the layer. To verify that there was still an HTL present in the double-layer device, we also performed optical absorption measurements, as shown in Figure 8. The absorption feature of the [PFO-BEHTPD]$_1$[PFO-TPD]$_7$ at 350 nm, which is not present in the MEH-PPV, is still clearly visible in the double-layer device. This demonstrates that deposition of the MEH-PPV layer does not dissolve the HTL when spin coated at room temperature. Because of the alignment of the HOMO levels of MEH-PPV and [PFO-BEHTPD]$_1$[PFO-TPD]$_7$ and the relatively large band gap of [PFO-BEHTPD]$_1$[PFO-TPD]$_7$, as schematically indicated in Figure 1, the electrons injected from the cathode into MEH-PPV will be blocked at the interface between the polymers. As a result, in the double-layer PLED, all of the light will be generated in the MEH-PPV layer. In Figure 9 the $J-V$ characteristics of the double-layer PLED is shown, together with the single-layer MEH-PPV-based PLED. To enable a direct comparison, we spin coated the MEH-PPV layer from the same solution. The $J-V$ characteristic of the double-layer PLED is slightly lower than the MEH-PPV single-layer device because of the extra voltage drop across the HTL. This voltage drop depends not only on the mobility and thickness of the [PFO-BEHTPD]$_1$[PFO-TPD]$_7$ HTL but also on the fact that the current in the HTL is space-charge-limited. This means that to fill the HTL with charge carriers and make it conductive, a certain voltage is required to electrostatically allow this space charge. In Figure 10, the efficiency (light output divided by current) is plotted for a PEDOT−PSS/MEH-PPV/Ba/Al and the double-layer PEDOT−PSS/ [PFO-BEHTPD]$_1$[PFO-TPD]$_7$/MEH-PPV/Ba/Al. The efficiencies are normalized to the maximum efficiency of the MEH-PPV-based PLED. We observe that at lower voltages the efficiency of the double-layer PLED rises more slowly with voltage as compared with the single-layer PLED. The increase in the efficiency with voltage is a direct consequence of the unbalanced charge transport in the PLEDs.[16]

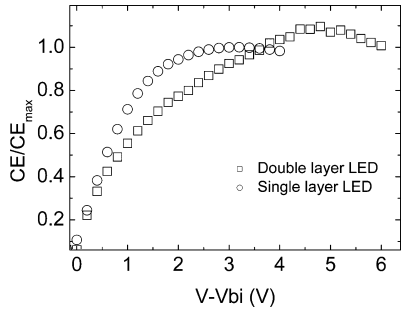

Figure 10. Normalized conversion efficiency (CE) (light output/current) of a single-layer MEH-based (○) and double-layer [PFO-BEHTPD]$_1$[PFO-TPD]$_7$/MEH-PPV-based (□) PLED.

The electron transport is strongly reduced as compared with the hole transport because of trapping effects. As a result, at low voltages, the light is mainly generated in a region close to the cathode, whereas at high voltages, when the electron traps are filled, the light is generated more homogeneously in the device. Because of the nonradiative recombination losses at the cathode interface, where a large number of exciton quenchers are present, the efficiency is strongly reduced at low voltages. The slower rise of the efficiency for the double-layer device is also a consequence of the additional voltage drop across the HTL. To fill the electron traps and reduce the quenching, a higher total voltage is required. At higher voltages, where the light is generated more homogeneously in the MEH-PPV layer, the efficiency of the double-layer device is 10% higher as compared with the single layer PLED. The presence of the HTL with its electron blocking functionality reduces the quenching of excitons at the PEDOT/PSS anode, thereby enhancing the efficiency.

4. Conclusions

In conclusion, we have reported on the synthesis and electrical characterization of polyfluorene−triarylamine copolymers with a tunable solubility. The room-temperature mobility amounts to $\sim 1 \times 10^{-10}$ m^2/(V s) and is not affected by the addition of nonsoluble derivatives. The [PFO-BEHTPD]$_1$[PFO-TPD]$_7$ HTL is insoluble in toluene at room temperature, enabling the construction of double-layer devices with MEH-PPV as active layer. These double-layer PLEDs exhibit a 10% higher efficiency at higher voltage because of a reduced exciton quenching at the PEDOT/PSS anode.

Acknowledgment. This work is part of the open technology program of the Technology Foundation STW. We thank B. Langeveld and I. Katsouras for the contributions to this work. Furthermore, technical assistance of J. Harkema and F. van der Horst is acknowledged.

References and Notes

(1) Tang, C. W.; VanSlyke, S. A. *Appl. Phys. Lett.* **1987**, *51*, 913.
(2) Burroughes, J. H.; Bradley, D. D. C.; Brown, A. R.; Marks, R. N.; Mackey, K.; Friend, R. H.; Burn, P. L.; Holmes, A. B. *Nature* **1990**, *347*, 539.
(3) D'Andrade, B. W.; Baldo, M. A.; Adachi, C.; Brooks, J.; Thompson, M. E.; Forrest, S. R. *Appl. Phys. Lett.* **2001**, *79*, 1045.
(4) Reineke, S.; Lindner, F.; Schwartz, G.; Seidler, N.; Walzer, K.; Lüssem, B.; Leo, K. *Nature* **2009**, *459*, 234.
(5) Greenham, N. C.; Moratti, S. C.; Bradley, D. D.; Friend, R. H.; Holmes, A. B. *Nature* **1933**, *365*, 628.
(6) Gong, X.; Wang, S.; Moses, D.; Bazan, G. C.; Heeger, A. J. *Adv. Mater.* **2005**, *17*, 2053.
(7) Domercq, B.; Hreha, R. D.; Zhang, Y. D.; Haldi, A.; Barlow, S.; Marder, S.; Kippelen, B. *J. Polym. Sci., Part B: Polym. Phys.* **2003**, *41*, 2726.
(8) Png, R.-Q.; Chia, P.-J.; Sivaramakrishnan, S.; Wong, L.-Y.; Zhou, M.; Chua, L.-L.; Ho, P. K.-H. *Appl. Phys. Lett.* **2007**, *91*, 013511.
(9) Rehmann, N.; Hertel, D.; Meerholz, K.; Becker, H.; Heun, S. *Appl. Phys. Lett.* **2007**, *91*, 103507.
(10) Tseng, S.-R.; Meng, H.-F.; Yeh, C.-H.; Lai, H.-C.; Horng, S.-F.; Liao, H.-H.; Hsu, C.-S.; Lin, L.-C. *Synth. Met.* **2008**, *158*, 130.
(11) Kim, J.-S.; Friend, R. H.; Grizzi, I.; Burroughes, J. H. *Appl. Phys. Lett.* **2005**, *87*, 023506.
(12) Park, J.-J.; Park, T.-J.; Jeon, W.-S.; Pode, R.; Jang, J.; Knon, J. H. *Org. Electron.* **2009**, *10*, 189.
(13) Tanase, C.; Wildeman, J.; Blom, P. W. M. *Adv. Funct. Mater.* **2005**, *15*, 2011.
(14) Redecker, M.; Bradley, D. D. C.; Inbasekaran, M.; Woo, E. P. *Appl. Phys. Lett.* **1998**, *73*, 1565.
(15) Campbell, A. J.; Bradley, D. D. C.; Antoniadis, H. *J. Appl. Phys.* **2001**, *89*, 3343.
(16) Blom, P. W. M.; Vissenberg, M. C. J. M. *Mater. Sci. Eng.* **2000**, *27*, 53.
(17) Tanase, C.; Meijer, E. J.; Blom, P. W. M.; de Leeuw, D. M. *Phys. Rev. Lett.* **2003**, *91*, 216601.
(18) Pasveer, W. F.; Cottaar, J.; Tanase, C.; Coehoorn, R.; Bobbert, P. A.; Blom, P. W. M.; de Leeuw, D. M.; Michels, M. A. J. *Phys. Rev. Lett.* **2005**, *94*, 206601.
(19) Craciun, N. I.; Brondijk, J. J.; Blom, P. W. M. *Phys. Rev. B.* **2008**, *77*, 035206.
(20) Koster, L. J. A.; Smits, E. C. P.; Mihailetchi, V. D.; Blom, P. W. M. *Phys. Rev. B.* **2005**, *72*, 085205.
(21) Craciun, N. I.; Wildeman, J.; Blom, P. W. M. *Phys. Rev. Lett.* **2008**, *100*, 056601.
(22) Holt, A. L.; Leger, J. M.; Carter, S. A. *J. Chem. Phys.* **2005**, *123*, 044704.

JP101079Y